Instruments and Methods

A simple and updated pneumatic method for uniaxial ice compression in the laboratory: experimental settings and creep test results on glacier ice

D. SAMYN,* M. DIERCKX, J.-P. REMY,† T. GOOSSENS, J.-L. TISON

Laboratoire de Glaciologie, Université Libre de Bruxelles, CP 160/03, Avenue F.D. Roosevelt 50, B-1050 Brussels, Belgium
E-mail: denis.samyn@geo.uu.se

ABSTRACT. Creep tests provide invaluable data to better understand the physical properties of ice under various conditions. We describe here a simple, updated pneumatic apparatus for experimental studies of ice rheological properties. The apparatus is designed to perform two simultaneous compression creep tests either in a cold room or in atmospheric conditions when coupled to an external cooling circulator. We present results from calibration tests of the apparatus and provide new data from creep tests performed on temperate glacier ice samples. These calibration and creep results show that the apparatus is able to provide fast and reliable mechanical ice characterization. The secondary creep rates measured in this study range between $1.59 \times 10^{-8}\,s^{-1}$ (at 0.21 MPa) and $4.38 \times 10^{-7}\,s^{-1}$ (at 0.71 MPa) at –10°C for quasi-isotropic ice, which is consistent with former standard published data. The corresponding mean parameter, *A*, is $5.20 \times 10^{-16}\,s^{-1}\,kPa^{-3}$, which also compares well with the range of reported other studies.

INTRODUCTION

Despite several decades of research since Glen's (1955) pioneering work on glacier ice deformation and the interdependence of stress, temperature and duration of creep, much remains unknown about the various types of microstructures produced in individual grains and the associated mechanical properties. Glaciers and ice sheets occur as polycrystalline aggregates, the behaviour of which is determined by the behaviour of individual grains in bulk. Therefore, to improve ice-flow models and make better predictions of polar reactivity against climate change, it is of particular interest to glaciologists and geophysicists to investigate the evolution of snow/ice crystal structures at microscales together with changes in strength, ductility and anisotropy, and to summarize these characteristics into simple rheological parameters through deformation experiments. This paper is also motivated by the fact that ice rheology, despite having brought an invaluable body of knowledge to geophysics, is a discipline of glaciology and material science that has lost momentum in the past 10 years, owing mostly to the time required to obtain proper and significant results. Various ideas and theories that have not always been based on good experimental data have also found their way into the literature. There is therefore a need today to revitalize laboratory studies of the rheology of ice.

In this context, we propose here a simple and updated method for conducting ice compression experiments in the laboratory. The simplest and most conventional method to date for ice compression experiments has been the 'static loading' method, in which a constant load is applied, either directly or by transmission through a lever arm, by a dead weight, to the sample. However, this advantage of simple use and design can be counterbalanced by a lack of versatility and control during the experiment. The method described here has been designed to meet the following requirements: (1) reasonable cost, simple construction and user-friendly structure, (2) data acquisition reliability, (3) ability to conduct simultaneous experiments over long time periods (months) and (4) upgrading potential. We first describe the concept of the experimental apparatus developed, then detail the results of bath cooling and ice deformation tests and finally propose some potential adaptations for upgrading.

COMPRESSION APPARATUS AND COOLING BATH

The compression apparatus described here has been designed to perform uniaxial compression tests under static load and unconfined conditions (Fig. 1). Equipped with two customized commercial driving units, it allows double, independent, simultaneous strain experiments. Load is provided by pneumatic drives (Festo™) with integrated (high-alloy steel, non-corrosive) guide rods. In order to meet our requirements regarding reproducibility and versatility in the range of loadings that can be applied, modifications have been brought to some piston factory settings as follows in order to lower friction along the rods: (1) The standard joints have been replaced with Viton® joints for a better glide along the rods and a better tolerance to changing laboratory conditions (temperature, humidity). (2) The standard guide rods have been replaced with X20CR13 stainless steel, with no surface treatment. (3) For the case where the compression apparatus is used in atmospheric room conditions (see below), the standard grease has been replaced with a high-temperature long-term grease (Barrierta L55/1) usually used in 'low friction' gas struts. (4) A piston aluminium front plate with the same dilatation coefficient as the piston body has been manufactured to prevent gripping along the rods (especially at low temperature) and thereby to

*Present address: Department of Earth Sciences, Uppsala University, Villavägen 16, SE-752 36 Uppsala, Sweden.

†Deceased.

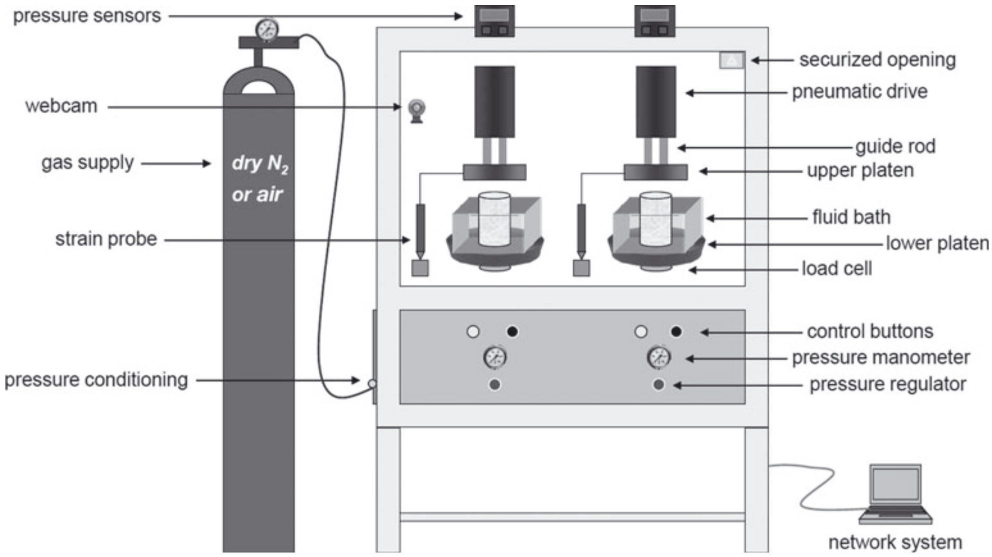

Fig. 1. Schematic of the experimental deformation apparatus.

secure parallelism of the guide rods through time. (5) Prior to use in the laboratory, the driving units have been subjected in the factory to intense running for 48 hours at the speed expected during our experiments.

The driving stroke of the compression units is 160 mm; the operating octahedral stress at the end of the piston line ranges from 0.075 MPa to >6 MPa, which for a 4 cm diameter sample, for example the experiments documented here, corresponds to minimum and maximum forces of 200 and >7500 N respectively. The maximum driving unit speed is 0.4 m s^{-1}. Gas can be delivered either by a pressurized gas reservoir or by a compressor, and the desired pressure is controlled by pressure regulators. Perbunan® rubbers, which resist low temperatures and show high resistance to wear and low permeability to gases, are used for the gas tubing connections. The frame structure of the rig is constructed of profiled aluminium elements that resist high load and can be easily assembled. This type of all-in structure ensures low-cost building and fast reshaping. The apparatus is suitable for deforming samples up to ~20 cm long and for measuring strains of several tenths of a per cent on centimetre-scale samples.

The apparatus structure can be used either at atmospheric temperature or in a cold-room environment. Sample temperature is controlled by the cold-room atmosphere itself or by immersion in a liquid bath connected to an external refrigerating system and driven by an internal pump (Julabo™) (Fig. 2). When the latter option is chosen, the cooling bath lies on a platen coupled to the load cell. The refrigerating circulators provide high cooling capacity, thereby ensuring rapid cool-down and stabilization of the circulating liquid. Silicone oil of low viscosity, low volatility

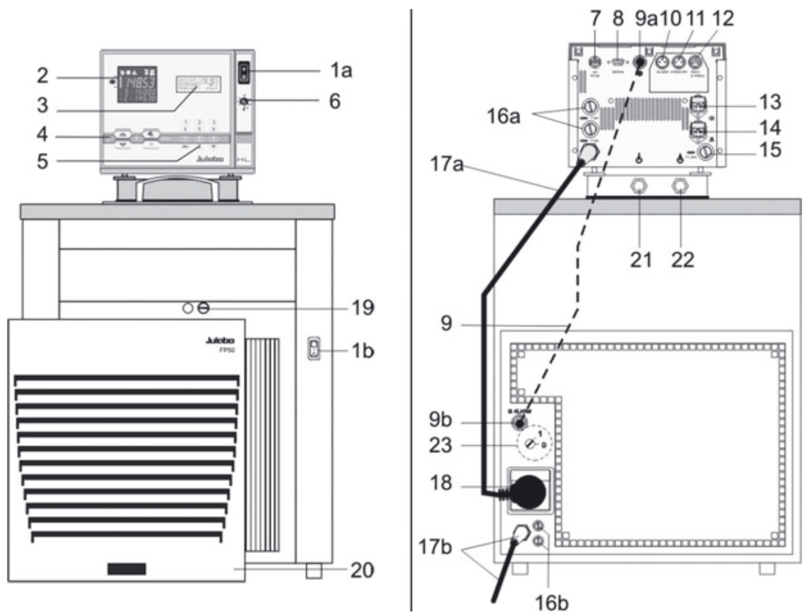

Fig. 2. Schematic of the cooling circulator (Julabo™): (left) front view; (right) rear view. Components of interest are detailed as follows: **2, 3:** header: control displays; **4, 5:** navigation keypads; **7:** socket for external measurement and control sensor; **9:** control cable for refrigerated circulator; **13, 14:** connectors for pumps or solenoid valve; **19:** drain screw with drain connection; **21, 22:** pump connections.

and low toxicity (Dow Corning™ 200, 10 cSt) is used as a cooling liquid (personal communication from T.H. Jacka, 2007). Advantages of this fluid are (1) it is non-toxic, (2) it protects the ice from ablation, (3) it is highly stable in experimental conditions and (4) it has reasonably good calorific capacity. Sample erosion by the circulating cooling oil has been tested and did not show any noticeable effect on long-term experiments.

Two main types of bath cooling systems are available nowadays for our purpose: circulation-induced cooling and conduction-induced cooling. Both systems have been tested in this work and have provided satisfying results at temperatures close to the melting point of ice. Circulation-induced cooling, however, showed faster temperature stabilization in these conditions. When temperature became significantly negative, typically a few degrees below the ice melting point, conduction-induced cooling showed more suitable characteristics, especially when the relative humidity of air in the vicinity of the cooling bath was at saturation. In this case, frosting on the walls of the bath can cause ice flakes to sink and accumulate in the cooling liquid and be either trapped in the cooling tubing or clustered on the cooling controllers, thereby affecting experimental efficiency.

One should notice that the deployment of an external cooling system as described above to control sample temperature is not mandatory if the entire compression rig can be hosted into a cold room capable of maintaining the temperature stability required for creep experiments (ΔT should typically be lower than 0.1°C, especially in the vicinity of the melting point, in order to minimize the influence on strain rate). Experience shows, however, that freezing atmosphere can have undesirable effects on the performance of pneumatic systems: (1) Since the state of gas present in the driving units is determined by the ideal gas law, any significant change in temperature will affect the gas volume and thus the load applied at the end of the driving unit. (2) If not properly accounted for in the design phase, low-temperature exposure can induce tightening and eventually gripping at various levels of the driving units (but mostly at the outer-cylinder-wall/guiding-rod interface) as a result of differential thermal expansion. This gripping can have a mechanical effect on piston load as well, particularly at driving loads close to the minimum afforded by the unit. We therefore suggest that an external cooling system such as that presented above should be favoured to maintain the required freezing temperature for creep, especially if the air-conditioning system in the cold room cannot guarantee temperature variations lower than 0.1°C and/or if the ambient air is not sufficiently dry (<40%) to prevent frosting on the unit walls. If the cold-room option is preferred we advise using nitrogen as the compression gas in the delivery line. When pressurized at experimental conditions, this gas shows a lower dew point than air in the cold room, thereby preventing condensation and further freezing in the tubing line and driving units. When used in ultra-dried form (0.5% vapour residual), experience shows that nitrogen efficiently minimizes the possibility of tubing obstruction by water vapour freezing. In addition, since nitrogen makes up most of the atmosphere, it reduces possibilities of leakage in the tubing and driving systems. According to the above, the advised minimum operating temperatures for the compression units to be used are in the range –15°C to –20°C in a properly controlled cold room (without the use of a cooling bath), and below –30°C in a properly conditioned STP (standard temperature and pressure) atmosphere using a cooling bath.

DATA ACQUISITION

Deformation of ice samples is measured using displacement transducers (Solartron™) with digital electronic output. The displacement sensors have an uncertainty between 0.1% and 0.2%, depending on their measurement range (2 and 5 mm respectively). Several digital probes can be used simultaneously in any combination by means of a network system (Orbit™) connected to a PC via a USB port. Each probe is plugged to the network through an individual interface module and is automatically given a unique address on installation. Compression load during an experiment is monitored by analogue load cells (Thames Side-Maywood™) connected to the digital network through analogue input modules. Precision temperature probes (Pt100) are similarly connected to the network. The uncertainties of load and temperature cells are 0.1 N and 0.01°C. Pressure gauges have been directly plugged into the inner chamber of the driving units to survey internal pressure variations and allow a better adjustment (e.g. to laboratory temperature change) of the load. Readings from the various sensors are acquired directly and simultaneously, allowing continuous data processing and experimental control. It is advisable to place the whole deformation apparatus on an anti-choc carpet to minimize the effect of ambient vibrations on data acquisition.

To allow monitoring of running experiments from remote places, the acquisition PC unit has been plugged into the internet network. Knowing that experiments may last up to several weeks or months, it is indeed convenient, once the experiment has been launched, to be able to check and process acquired data remotely. A webcam device has also been installed in the vicinity of the system for the same monitoring reasons.

SECURITY ISSUES

Working with pneumatically driven units involves serious security issues, mostly as a result of the high-impact potential of the driving units. To avoid any possibility of corporal damage during our experiments, the compression apparatus has been equipped with several security items. First, the rig frame has been closed with clear plastic sheets to limit direct physical contact with the pneumatic drives. Second, the opening of the frame box door is operated by coded electromagnets. Opening the door (and thus deactivating the electromagnets) while the drives are pressurized has the effect (through a solenoid valve) of (1) automatically cutting gas supply and (2) flushing out the gas contained in the driving system. Reactivation of the driving units can then be done (through a reset button) only when the door is closed again. Third, the gas delivery line has been equipped with anti-return valves to prevent the platens of the pneumatic drives from falling off when the line is flushed out. Finally, progressive pressurization of the pneumatic drives is imposed on start by soft-start valves at the beginning of the line.

To ensure sensor and sample security, webcams have been installed in the vicinity of the ice samples to detect remotely the potential development of cracks in the ice, and thereby to prevent sensor destruction as a result of piston

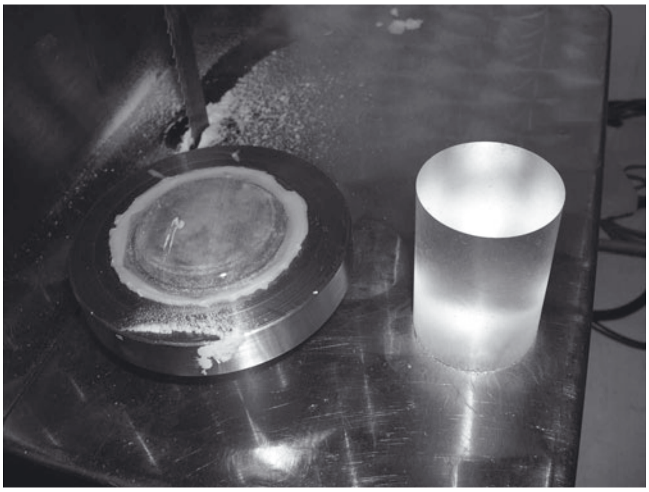

Fig. 3. Ice sample after shaping and its holder. The scale is given by the ice cylinder height (~6 cm).

fall-off. A webcam can also be used in the vicinity of the external freezing bath to remotely monitor the level of cooling liquid in the external bath, and thereby guarantee sample durability.

SAMPLE SHAPING AND PREPARATION TIPS

Prior to deformation, ice samples must be shaped (Fig. 3). Conventionally, to ensure homogeneous deformation without barrelling or buckling during compression, two conditions must be fulfilled: (1) The sample slenderness ratio (height/diameter) should range between ~1 and ~3 (preferably closer to 3; Bieniawski and Bernede, 1979). (2) The ratio of the sample diameter to the mean linear ice grain size should be at least 10 (Wojtkowiak, 1978). For the validation deformation experiments described below (mean grain size 1.6 mm), a slenderness ratio of ~2 has been selected as a standard in this work. This corresponds to a ratio of sample diameter to grain diameter of ~25. Shaping is achieved with the aid of a customized commercial lathe to obtain sharp and properly oriented sample edges and faces. Our lathe chuck has been upgraded with soft concave jaws to maintain the sample, smoothly but firmly, along the shaping axis. A dynamometric wrench has also been mounted on the jaw-tightening system to allow soft, progressive, secure sample installation on the chuck. Speed rotation of the lathe axis and advancing speed of the cutting tool are coupled and can be modulated precisely, depending on the ice mechanical characteristics, to ensure sharp and strainless shaping. Typical speed rotation used in this set of experiments was 320 rotations per minute.

Before an experiment begins, a Teflon sheet is inserted between the flat faces of the specimen and the piston platens in order to prevent gripping and also to limit inhomogeneous deformation effects at the outer surface of the test sample (Hsu, 1979).

RIG CALIBRATION AND TESTING

Various tests have been performed in order to calibrate the compression apparatus. Only results from experiments where the rig is used int atmospheric conditions and coupled with an external cooling system are described here, corresponding to the most advanced settings tested.

Being essentially composed of metallic components, during operation the compression apparatus undergoes an intrinsic (mostly elastic) deformation that should be subtracted from the ice creep data. In Figure 4, results are shown from an experiment where pressure has been applied for several hours and at various intensities on a plain steel block of well-known Young's modulus ($E = 2.1 \times 10^5$ MPa). In this way, deformation of the steel sample can be calculated and subtracted from the total strain measured, thereby yielding the internal deformation due to the apparatus at a given applied stress. The latter appears to increase regularly at applied stress lower than 0.06 MPa,

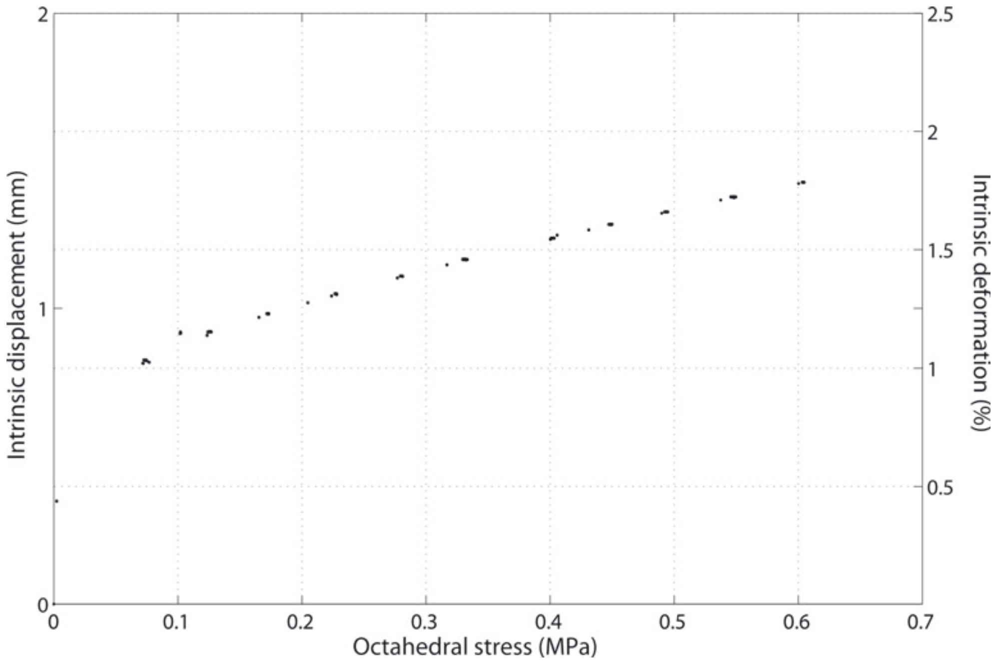

Fig. 4. Observed intrinsic deformation and displacement of the apparatus versus applied octahedral stress.

Table 1. Statistical parameters for the experiment illustrated in Figure 5

	Pressure applied MPa	Pressure corrected MPa
Mean	0.362	0.362
Max	0.374	0.370
Min	0.355	0.355
Delta	0.019	0.015
Std dev.	0.053	0.038
Error (%)	6.6	4.0

before reaching an asymptotic value above 0.06 MPa. However, such behaviour is expected to evolve in an unpredictable way across time, depending on the way the whole apparatus wears. Therefore, such a calibration of the intrinsic apparatus deformation is to be carried out on a regular basis.

Stability of applied stress during an experiment is also important for precise creep experiments. Results from a compression test lasting for about a week under uncontrolled atmosphere (temperature and pressure) and with an applied stress of ~0.36 MPa are shown in Figure 5. A statistical table for this experiment is provided in Table 1. Figure 5a shows that, despite the presence, for security reasons, of a soft-start valve at the beginning of the compression line, the effective pressure on the piston platen stabilizes almost instantaneously (Table 1) and varies within a narrow range once the experiment is launched. It also illustrates the close relationship between pressure in the piston and the air temperature as expected from the ideal gas law. Using the experimental P/T relationship from the data shown in Figure 5a, we can use the regression equation, $P = -0.041 * T + 4.7$ (Fig. 5b) to correct this temperature bias on the pressure, as illustrated in Figure 5c. The results of this experiment are interesting for two main reasons. First, they testify to the excellent reactivity of the driving units to any change in experimental conditions during deformation (e.g. temperature variations or vertical shortening of the sample). Second, they further emphasize the need for stable air temperature during an experiment. Pressure variations in the experiment shown in Figure 5 would barely have been noticeable had the laboratory atmosphere been conditioned.

Table 2. Statistical parameters for the experiment illustrated in Figure 6

Programmed T (°C)	–10.00
T max (°C)	–9.93
T min (°C)	–10.04
Delta (°C)	0.11
Mean (°C)	–9.99
Std dev.	0.03

The reliability of the temperature-conditioning system at the end of the cooling chain, i.e. in the sample vicinity, can be appraised from the cooling-bath conditioning experiment illustrated in Figure 6 and Table 2, where a temperature of –10.00°C was initially programmed on the cryostat. Temperature variations of only a few hundredths of a °C (associated here with a slight diurnal cycle) are noticeable in the cooling bath despite unconditioned atmospheric temperature in the laboratory (Table 2), which means that the effect of our cryostatic method on sample deformation can be considered negligible.

DEFORMATION RESULTS

Deformation tests have been conducted to verify the efficiency of our apparatus in deforming ice specimens. These tests have been performed on ice-core samples collected in October 2007 and 2008 in the accumulation zone of Glacier de Tsanfleuron, Switzerland (46°20′ N, 7°13′ E). The samples are typical of the transition zone between firn and ice, as indicated by their (1) high bubble content, (2) intermediate density (mean 870.1 kg m^{-3}), (3) millimetre-size ice crystals (mean ~1.6 mm) and (4) quasi-isotropic crystal orientation. In Figure 7, results from compression tests at –10°C on these glacier ice samples are compared with results obtained from similar experiments on isotropic artificial ice by Jacka (1984). Note that, as illustrated in Table 3, some of the samples were subjected to stepwise increasing load until secondary creep was reached, in order to deduce the flow index n in Glen's law, $\dot{\gamma}_{xy} = A\tau_{xyn}$, where $\dot{\gamma}_{xy}$ is the shear strain rate, A is a factor dependent on temperature, crystal orientation, impurity content, etc., τ_{xy} is the shear stress and n is a constant. The measured octahedral secondary creep rates (Table 3) range

Table 3. Characteristics of the ice specimen (similar, isotropic c-axis fabric) deformed at –10°C

Sample ID	Stress MPa	Oct. stress MPa	Min. strain rate s^{-1}	Oct. min. strain rate s^{-1}	Mean crystal size cm	A factor s^{-1} kPa^{-3}
A47a	0.70	0.33	4.48×10^{-8}	2.59×10^{-8}	0.14	3.02×10^{-16}
A49a	0.70	0.33	6.50×10^{-8}	3.75×10^{-8}	0.17	4.37×10^{-16}
A47b	0.45	0.21	2.75×10^{-8}	1.59×10^{-8}	0.16	7.47×10^{-16}
A47b	0.67	0.31	7.07×10^{-7}	4.08×10^{-8}	0.16	5.62×10^{-16}
A47b	1.05	0.50	3.98×10^{-7}	2.30×10^{-7}	0.16	7.48×10^{-16}
A47b	1.30	0.61	1.00×10^{-6}	5.77×10^{-7}	0.16	9.56×10^{-16}
A47c	0.64	0.30	3.98×10^{-8}	2.30×10^{-8}	0.18	3.56×10^{-16}
A47c	1.02	0.48	1.58×10^{-7}	9.15×10^{-8}	0.18	3.21×10^{-16}
A47c	1.27	0.60	3.16×10^{-7}	1.83×10^{-7}	0.18	3.26×10^{-16}
A47c	1.50	0.71	7.58×10^{-7}	4.38×10^{-7}	0.18	4.63×10^{-16}

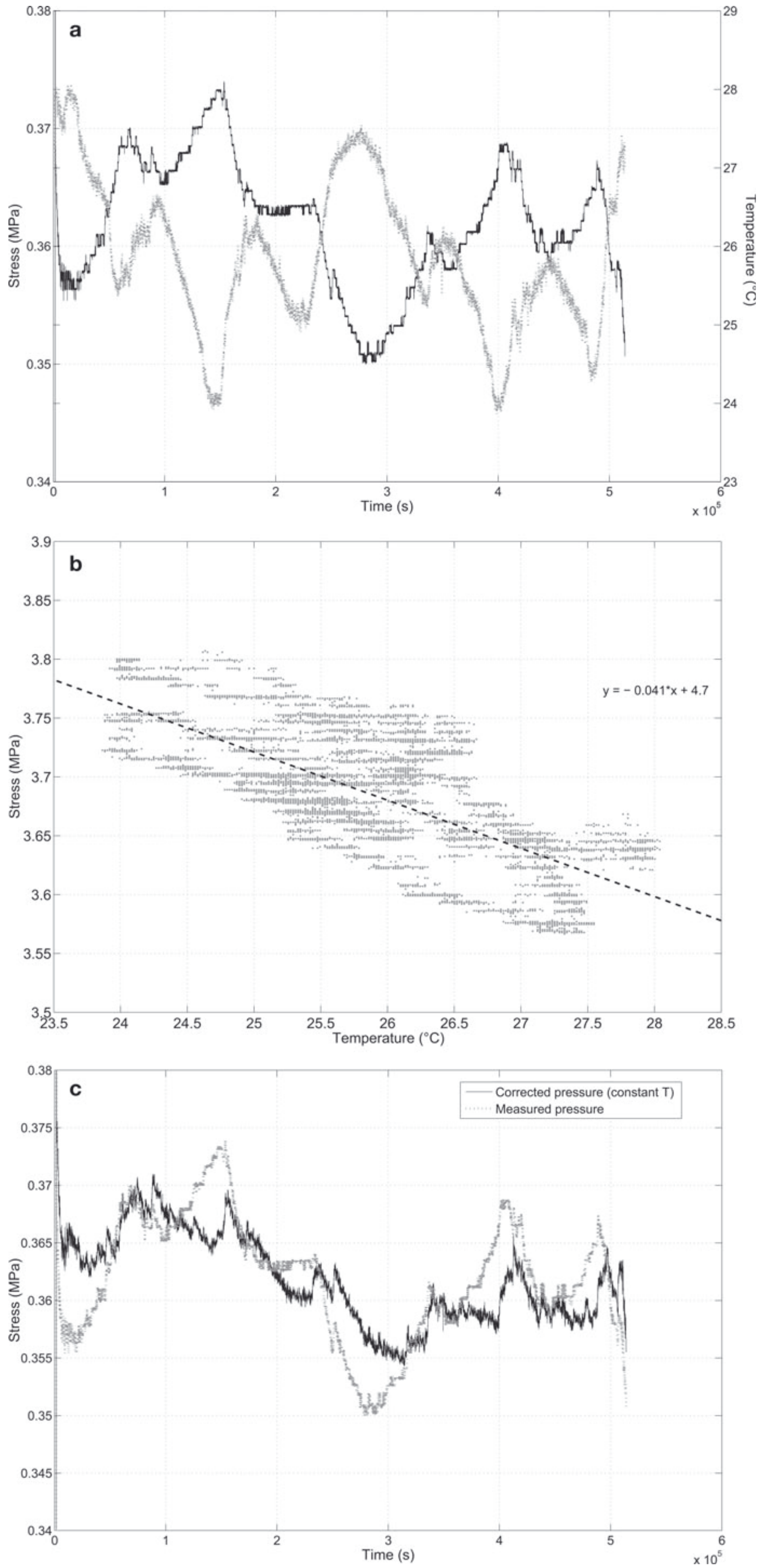

Fig. 5. Compression test under unconditioned laboratory atmosphere: (a) pressure in the piston chamber vs laboratory temperature diagram ($r^2 = -0.7$); (b) regression diagram of the piston-chamber pressure vs laboratory temperature; (c) piston pressure curve corrected for atmosphere temperature variations. See Table 1 for statistics.

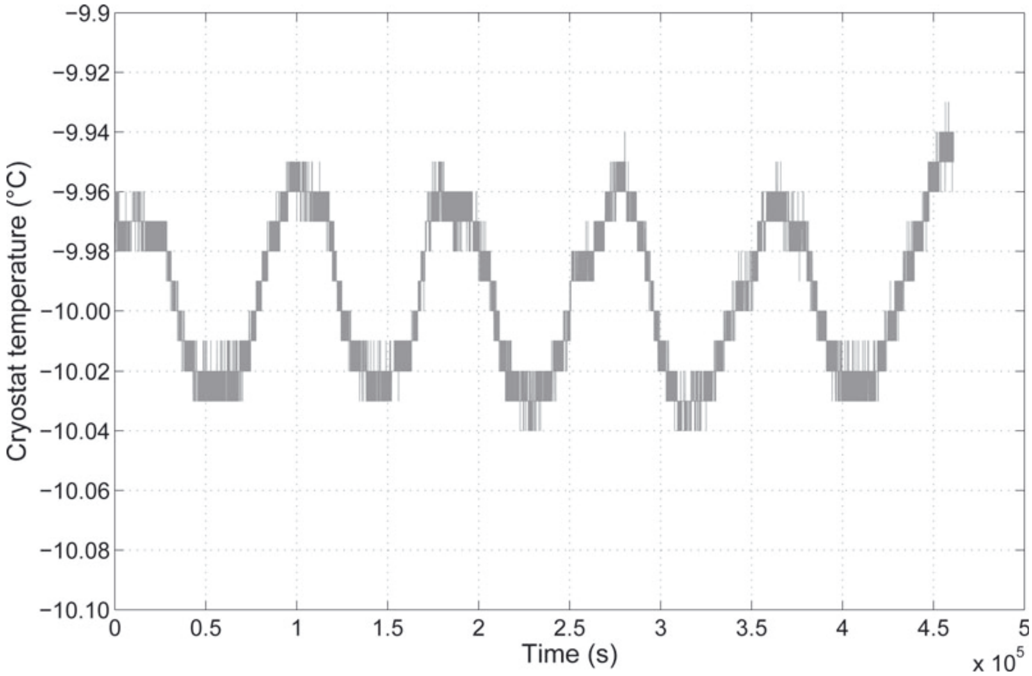

Fig. 6. Results from a temperature-conditioning experiment of the cooling bath (~5.3 days) at an initially programmed temperature of –10.00°C. See Table 2 for statistics.

between 1.59×10^{-8} s^{-1} (at 0.21 MPa) and 4.38×10^{-7} s^{-1} (at 0.71 MPa), which is consistent with creep data from Jacka and other standard published data (e.g. Paterson, 1994). Interestingly, Figure 7 shows that our results are aligned on a slope ($n = 3.15$) parallel to that of Jacka ($n = 3$), but with a higher intercept (or A parameter). Yet the average fluidity parameter A obtained in this study (5.20×10^{-16} s^{-1} kPa^{-3}) falls into the range reported from other studies (3.0–8.7 $\times$ 10^{-16} s^{-1} kPa^{-3}) by Paterson (1994), whereas the average A calculated from Jacka's data (4.0×10^{-16} s^{-1} kPa^{-3}) on artificial ice falls into the lower part of this range. This slightly higher fluidity can be accounted for by the higher bubble

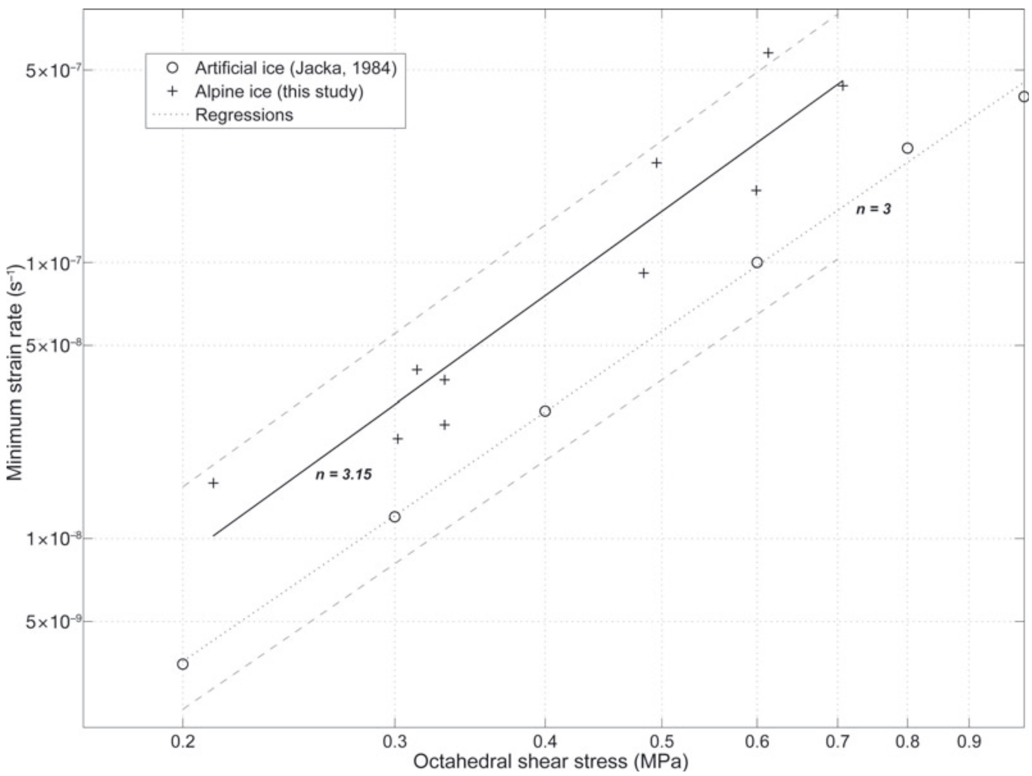

Fig. 7. Result comparison between deformation experiments on glacier ice samples (Glacier de Tsanfleuron, this study) and experiments on isotropic artificial ice by Jacka (1984). The bold correlation line represents this study ($n = 3.15$), the dotted line represents Jacka's data ($n = 3.00$), and the dashed lines give the range of creep data compiled by Paterson (1994).

content and/or salinity in our samples. Note that the lower correlation in this study can mostly be explained by the fact that our samples, being of natural origin, are more prone to differences in physical–chemical characteristics (e.g. slight fabric changes).

POSSIBLE ADAPTATIONS

The compression unit has been designed to host, if necessary, input and output arrangements for a programmable logic controller (PLC). A PLC is a real-time electronic system used for automation and with which output steps can be followed in response to input conditions within a bounded time. The potential applications of such a system to our purpose are the prevention of unintended operations that could damage either the equipment or the ice sample, and the automation of tedious/time-consuming tasks, such as cyclic loading. Experience will show whether it is necessary to upgrade our compression unit with such a device.

Duval (1978) and Li and others (1996), for instance, have demonstrated the importance for ice mechanics studies of creep tests in combined stress configurations. To allow the upgrade of our compression device with a torsion option, a ring made up of phosphorous bronze has been mounted underneath the lower platen of both deformation units. This special alloy, notable for its toughness and low-friction coefficient, will limit the friction of the lower platens on their supports when rotating. The desired torque for the platens can then easily be provided by coupling their bases to a belt driven by a controllable rotor or dead weights.

CONCLUSION

We have developed a simple pneumatic apparatus, customized from mass-produced units, capable of conducting two different uniaxial compression tests simultaneously. The apparatus can be used either in STP atmosphere conditions if coupled with a cooling circulator, or in a cold room if temperature variations and humidity in the room can reasonably be controlled. Both ice specimens can be subjected to identical or different temperatures as needed. Original data from creep tests performed on glacier ice samples show excellent agreement with previously published data, thereby testifying to the efficiency and reliability of the apparatus.

ACKNOWLEDGEMENTS

This paper is a contribution to the Belgian Research Programme on the Antarctic (Belgian Federal Science Policy Office), project No. EA/11/3A ‘Belgian Ice Sheet – Shelf Ice Measurements in Antarctica (BELISSIMA)’. D.S. is currently funded through a Marie Curie Intra-European Fellowship, and M.D. through the IceCubeDyn project (Academic Research Collaboration) by the Communauté Française de Belgique (Belgium). We thank the Chief Editor T.H. Jacka and two anonymous reviewers for their helpful comments.

REFERENCES

Bieniawski, Z.T. and M.J. Bernede. 1979. Suggested methods for determining the uniaxial compressive strength and deformability of rock materials: Part 1. *Int. J. Rock Mech. Min. Sci. Geomech. Abstr.* **16**(2), 138–140.

Duval, P. 1978. Anelastic behaviour of polycrystalline ice. *J. Glaciol.,* **21**(85), 621–628.

Glen, J.W. 1955. The creep of polycrystalline ice. *Proc. R. Soc. London, Ser. A,* **228**(1175), 519–538.

Hsu, T.C. 1979. A study of the compression test for ductile materials. *Mater. Res. Standards,* **9**(12), 20.

Jacka, T.H. 1984. The time and strain required for development of minimum strain rates in ice. *Cold Reg. Sci. Technol.,* **8**(3), 261–268.

Li, J., T.H. Jacka and W.F. Budd. 1996. Deformation rates in combined compression and shear for ice which is initially isotropic and after the development of strong anisotropy. *Ann. Glaciol.,* **23**, 247–252.

Paterson, W.S.B. 1994. *The physics of glaciers. Third edition.* Oxford, Elsevier.

Wojtkowiak, F. 1978. Comportement mécanique d’une micrite et d’une granodiorite. Contribution à l’étude de la fissuration provoquée par sollicitations mécaniques. (PhD thesis, Université d’Orléans.)

MS received 3 June 2010 and accepted in revised form 26 November 2010